

BEHAVIORS OF CIRCULAR CONCRETE ENCASED COMPOSITE COLUMNS USING STEEL PLATE

ỨNG XỬ CỦA CỘT TRÒN HỖN HỢP BÊ TÔNG CỐT CỨNG SỬ DỤNG THÉP TẮM

Phan Dinh Hao

University of Science and Technology, The University of Danang, Vietnam

Currently PhD. Candidate at The University of Wollongong, New South Wales, Australia

E-mail: phandinhhao2008@gmail.com; dhp629@uowmail.edu.au

ABSTRACT

This paper investigates the effect of different structural steel configurations on the load carrying capacity of circular composite columns using steel plate through testing nine specimens. The specimens were divided into three groups of three specimens. The specimens of the first group, normal reinforced concrete columns, served as references. While the specimens of the two remaining groups were designed in two different configurations of steel plates, namely lateral reinforcement combined with steel plates (Group 1) and open bolt-connected steel plates (Group 2), respectively. Three specimens in each group were tested as columns with eccentricities of 0 (concentric), 25 mm and 50 mm. The columns' failure mechanisms were investigated in order to determine the strength, ductility and buckling of structural steel in columns. The study showed that Group 1 presented the greatest strength and ductility due to the effect of confinement by the helix and structural steel plates. Meanwhile, the strength and ductility of columns in Group 2 were not as high as expected due to the local buckling of structural steel and premature separation between the cover concrete and steel core.

Key words: circular encased composite columns; structural steel configuration; steel plate; columns' failure mechanisms; strength and ductility

TÓM TẮT

Bài báo này nghiên cứu ảnh hưởng bởi việc phân bố cấu tạo khác nhau của cốt cứng đến khả năng chịu tải của cột composite hình tròn dùng thép tấm thông qua thử nghiệm 9 mẫu cột, được chia làm ba nhóm mỗi nhóm có 3 mẫu. Các mẫu trong nhóm thứ nhất là cột bê-tông cốt thép thường, dùng làm tham chiếu. Các mẫu của hai nhóm còn lại được thiết kế theo 2 kiểu cấu tạo cốt thép tấm khác nhau, cụ thể là cốt thép tấm kết hợp với cốt đai và cốt thép tấm liên kết hồ bằng bu-lông. Các mẫu trong mỗi nhóm được thử với tải lệch tâm 0, 25 mm và 50 mm. Nghiên cứu cho thấy nhóm cột LCP có cường độ và độ dẻo cao nhất do cấu tạo cốt thép hợp lý trong tiết diện và ảnh hưởng giam giữ bê tông nhờ cốt đai xoắn và thép tấm. Cường độ và độ dẻo của nhóm cột OBP không cao so với tính toán là do hiện tượng mất ổn định cục bộ của lõi thép và sự tách sớm giữa vỏ bê-tông và lõi thép.

Từ khóa: cột tròn bê-tông cốt cứng; cấu tạo thép kết cấu; thép tấm; cơ chế phá hoại cột; cường độ và độ dẻo

1. Introduction

The load-carrying capacity of composite columns had been investigated by many researchers. Razvi and Saatcioglu [1] studied the behavior of circular high-strength concrete columns and reported that using helix in reinforced concrete columns significantly increases both their strength and ductility. In addition, Hadi [2, 3] used Fiber Reinforced Polymers (FRP) to strengthen plain concrete and high strength reinforced concrete columns subjected to eccentric compression loading and

found that using Carbon FRP is more effective than Glass FRP in increasing the strength and ductility of columns. Another study [4] investigated the benefits of using different types of mesh to reduce cover spalling of high-strength concrete columns. More other studies focused on the analysis of the load capacity of composite columns. The concrete filled steel columns have advantages of full usage of materials and reduction of construction cost due to the steel section acting as permanent formwork. However, concrete encased steel columns have a better performance in corrosion and fire resistance than

that of concrete filled steel ones [5]. Most columns used in building structures are made of rectangular or square sections. For rectangular encased composite columns, researchers undertook both experimental and theoretical studies for short and slender columns [6-10]. These studies focused on analytical modeling and simulation to predict the axial capacity, flexural stiffness, strength, ductility and stability of concrete encased composite columns subjected to different loading conditions.

The strength and ductility are two substantial properties of concrete encased composite columns. The current standards [11-13] provide guidelines to analyze and design composite columns. However, there were discrepancies [6, 8] in calculation approaches and analysis results between those standards. El-Tawil and Deierlein [6] reported that ductility of composite columns depends on the concrete strength, the confined reinforcement, structural steel ratio and loading conditions. Mirza and Tikka [7] proposed new *EI* equations for slender concrete encased composite columns. Mirza and Lacroix [8] investigated the discrepancies of strength analysis of rectangular concrete encased steel composite columns using different standards and showed that Eurocode-4 [11] computes the column strengths more accurately than other computational procedures. Chen and Lin [9] conducted a study predicting the axial load-carrying capacity of concrete encased steel composite columns and reported that partial confinement factor is highly dependent on the lateral tie spacing, while the shape of structural steel section affects the high confinement factor of concrete.

There exists an extensive literature on circular concrete filled steel columns, meanwhile few studies on circular encased composite columns have been carried out [14]. Hence, this study investigates loading capacities of the latter columns with different structural steel configurations mainly based on an experimental program. The idea of combination of steel plates on the composite column sections is presented herein, including lateral reinforcement combined

with steel plates (LCP) and open bolt-connected steel plates (OBP) groups compared to the reference group (NR). The strength, ductility and steel buckling issues of all specimens in the three groups are considered in detail. The columns' load-carrying capacities derived from the experimental program are determined to evaluate influences of structural steel configuration on the column behaviors.

2. Experimental Program

2.1. Design of Specimens

In this study, nine circular columns with different steel configurations were cast for testing. All columns were 900 mm in height and 209 mm in diameter. The columns were made of normal strength concrete with a nominal compressive strength of 32 MPa. Concrete cover was maintained at 24 mm thickness on the surrounding surface and 20 mm at the top and bottom of the columns. For Group NR, the reinforcement of specimens was designed according to AS 3600-09 [15], which included 6 N12 longitudinal deformed bars and a helix of R8@60 plain bar with nominal tensile strengths of 500 MPa and 250 MPa, respectively. For Group LCP, the structural steel of three specimens was made of steel plates (90x6) x6m long, and a helix of R8@60 was used as lateral reinforcement. The specimens of Group OBP were reinforced in a similar way as the specimens of Group LCP, but their lateral reinforcement was changed to bolt-connection with three D10 bolts at 330 mm spacing along each corner. The structural steel designed in LCP and OBP specimens with a steel ratio according to ACI 318-02 [13], has a nominal tensile strength of 320 MPa. Details of dimensions and steel configuration in the cross sections of all specimens are shown in Figure 1.

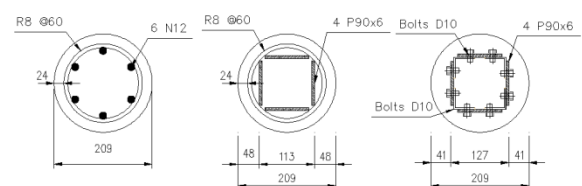


Figure 1. Cross-section details of the specimens

2.2. Test Configuration

The specimens were divided into three groups: NR, LCP and OBP as mentioned above. From each group, the first specimen was tested under a concentric compression loading, while the second and the third specimens were tested under eccentric compression loading with an eccentricity of 25 mm and 50 mm, respectively. A detailed test matrix of the experimental program is given in Table 1. All specimens were labeled with the respective group name and the loading condition in which the specimen is tested, where the number stands for the load eccentricity. The two label parts are connected with a hyphen, for instance, NR-25 represents the specimen in Group NR, which was tested under 25 mm eccentric loading, or LCP-50 stands for the specimen in Group LCP that was tested under 50 mm eccentric loading.

Table 1. Test matrix of the experimental program

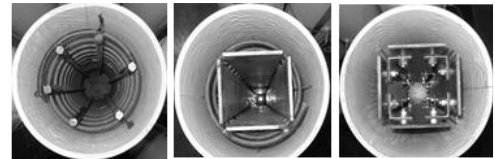
Specimen	Steel Bars		Steel Plates	Eccentricity
	Lateral	Longitudinal		
NR - 0	R8@60	6N12	None	0
NR - 25	R8@60	6N12	None	25 mm
NR - 50	R8@60	6N12	None	50 mm
LCP - 0	R8@60	None	4 P90x6	0
LCP - 25	R8@60	None	4 P90x6	25 mm
LCP - 50	R8@60	None	4 P90x6	50 mm
OBP - 0	None	None	4 P90x6 + Bolts	0
OBP - 25	None	None	4 P90x6 + Bolts	25 mm
OBP - 50	None	None	4 P90x6 + Bolts	50 mm

2.3. Preparation of Specimens and Preliminary Tests

The details of steel cage setup for three groups are shown in Figure 2. All specimens were cast using ready-mixed concrete supplied by a local company and then cured in room temperature condition for 28 days before they were tested.

The preliminary tests for steel and concrete samples were conducted at the High Bay Laboratory in order to determine the tensile strengths of the deformed bars, plain bars and steel plates, and the compressive strength of

concrete. The N12 deformed bars had average yield strength of 553.7 MPa, while the average yield strength of R8 plain bars was 636.3 MPa and it was 337.9 MPa for the steel plates (90x6). Concrete compression tests were carried out on each group of three cylinders in accordance to AS 1012.8 [16]. The average cylindrical compressive strengths of concrete at 7 days, 28 days and testing date were 22,33 and 34.5 MPa, respectively.



(a) Group NR (b) Group LCP (c) Group OBP

Figure 2. The configuration and position of steel cages in formworks

2.4. Testing of Specimens

All specimens were tested using the Denison 5000 kN compression testing machine in the High Bay Laboratory. For concentric loading, it was simple to set up the column into two steel loading heads. A specific loading system was used in order to conduct the eccentric compressive tests. The loading system consists of two steel loading heads with a gauge on top and two top steel plates. The gauges are 25 mm and 50 mm off center and the top overhang edge is placed in the gauges in order to create 25 mm and 50 mm eccentricity, respectively. Figure 3 depicts the details of the concentric and eccentric loading systems.

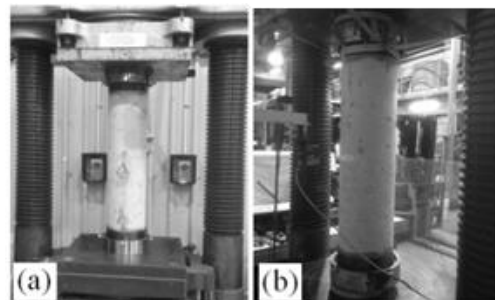


Figure 3. The concentric loading system (a) and eccentric loading system (b)

Before mounting the specimens on the testing machine, all columns were capped at both ends using high strength plaster to ensure even distribution of forces. A curing time of 30

minutes was given before the specimen was capped by the top loading head. Calibration was carried out to ensure leveling of the specimen by checking the centerline of the testing machine against the centerline of the load heads.

A linear variable differential transformer (LVDT) located on the bottom loading platform of the testing machine was used to measure the axial displacement of the specimens. For eccentric loading tests, a laser triangulation sensor was placed at mid-height of the specimen to measure the lateral displacement. The tests were deflection-controlled with a loading rate of 0.5 mm/min and the result data were recorded by a computer.

3. Experimental Results and Discussion

3.1. Summary of Test Results

Table 2 summaries the test results of all tested specimens. Comparing to the reference columns (Group NR), all LCP and OBP specimens showed an increase in ultimate load under compressive loading conditions; in particular, Group LCP outperformed the other groups in terms of ultimate load carrying capacity. Specimens subjected to eccentric loading showed lower ultimate load compared to specimens under concentric loading. Notably, in eccentric loading conditions, the lateral displacement of the specimens in Group LCP at the ultimate load was significantly larger than that of the other specimens, which indicates that the ductility of Group LCP was considerably bigger than the other groups.

Table 2. Summary of Test Results

Specimen	Yield Load (kN)	Ultimate Load (kN)	Axial Deflection at Ultimate Load (mm)	Lateral Deflection at Ultimate Load (mm)	Ultimate Moment (kNm)
NR-0	1020	1146	2.27	-	-
LCP-0	1356	1445	3.58	-	-
OBP-0	1062	1189	3.76	-	-
NR-25	680	729	3.48	2.92	20.354
LCP-25	772	859	4.50	3.76	24.705
OBP-25	700	757	3.04	2.89	21.113
NR-50	410	465	3.09	3.44	24.850
LCP-50	521	587	3.78	5.67	32.678
OBP-50	477	539	3.07	3.97	29.090

3.2. Failure Mechanism of Tested Columns

For columns under concentric loading, Specimens NR-0 and LCP-0 experienced a similar fracture mechanism. After the columns reached their peak load, cover concrete spalled leading to a decline of axial load. Next, the hardening period occurred as the concrete was confined by the helix. Then, the fracture of a helical ring occurred at the middle of the column for Specimen NR-0 and near the bottom of the column for Specimen LCP-0. The local buckling of the longitudinal reinforcing bars and steel plates in these positions occurred. The crushing of concrete core then happened, and finally the columns failed. Specimen OBP-0 witnessed a different fracture mechanism from the above two specimens, except the elastic behavior stage. This specimen failed early due to the buckling of the steel plates on the upper half of the column and the premature separation between the steel plates and the concrete. There was no hardening period during the testing process of Specimen OBP-0. The failure modes of Specimens NR-0, LCP-0 and OBP-0 are shown in Figure 4.

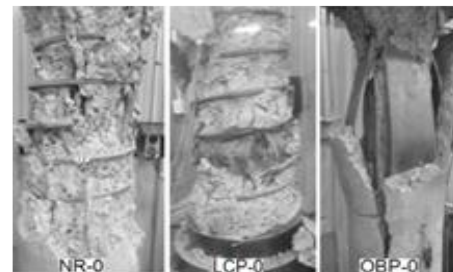


Figure 4. Failure modes of specimens under concentric loading

For 25 mm eccentric loading, the cover concrete of Specimen NR-25 spalled along the column on the compressive side, after reaching its ultimate load. The deformation of the column caused axial and lateral deflections, which led to an axial load decrease during this stage. After a short hardening, the column began failing due to larger lateral deflection. Specimen LCP-25 had a failure mechanism nearly similar to the reference one. However, the concrete spalling occurred at the upper half of the column. Specimen OBP-25 experienced an elastic behavior period and gained the peak column resistance. Shortly after that, the cover concrete spalled due to the deformation of

the steel plate on the side for 25 mm off center loading. Next, the lateral deflection of the column increased significantly, which led to the full cover concrete spalling, and the buckling of steel plates at the lower half of the column. Both Specimens LCP-25 and OBP-25 failed after reaching the peak load without a hardening stage.

For 50 mm eccentric loading, there was a difference of the failure mode between the specimens. The reference specimen (NR-50) presented a special failure mode, in which the lower two third length of the column had a small lateral deflection and the failure happened only near the top of the column. At this position, the cover concrete spalled and wider lateral cracking increased on the compressive and tensile sides of the column, respectively. This failure mode may have resulted from the relative movement of the top loading point compared to the bottom loading point or from the local weakness of the top column section. Specimen LCP-50 experienced a fracture mechanism roughly similar to Specimen LCP-25 but with larger deflections on both the horizontal and vertical directions. The spalling and lateral cracks developed from the top to the middle of the column, and tiny lateral cracks occurred on the lower half of the column. Specimen OBP-50 witnessed some lateral cracks at the top and the middle on tensile side of the column. Then, the buckling of a steel plate incidentally happened on the upper half of the column, after reaching its ultimate load. Next, the width of lateral cracks at top and middle of the column dramatically increased leading to the development of other vertical cracks around the column. The steel plates continued buckling at other positions and the separation between the cover concrete and the steel widely spread. Finally, the column failed after much more deflection and concrete fracture occurred. Figure 5 shows the failure modes of the specimens under eccentric loads of 25 mm and 50 mm, respectively.

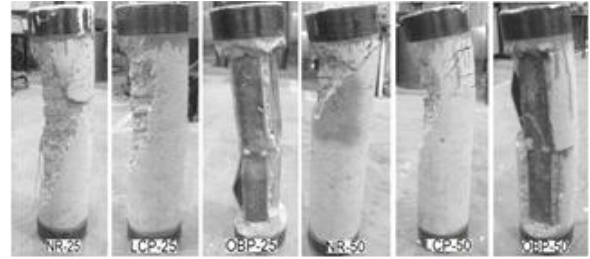


Figure 5. Failure modes of specimens under 25 mm and 50 mm eccentric loading

3.3. Load-deflection Diagrams

Figure 6 shows the load-deflection diagrams of all specimens of the three groups with different loading conditions. It can be seen that all the specimens showed a similar behavior during the first stage of loading before yield. Four specimens, namely NR-0, LCP-0, NR-25 and NR-F, had their hardening branch after yield and ultimate points of loading. The other specimens showed only a descending branch after achieving their peak load capacities. For compression loading, specimens in Group LCP had the highest strength. The ultimate load of Specimens LCP-0, LCP-25 and LCP-50 increased 26.1%, 17.8% and 26.2%, respectively, compared to the reference specimens. However, the results indicated that both Specimens LCP-F and OBP-F had lower strengths compared to the reference specimen for the flexural loading condition. It maybe depends on the concrete bonding and slips between concrete and steel plates occurring due to the increase of loading.

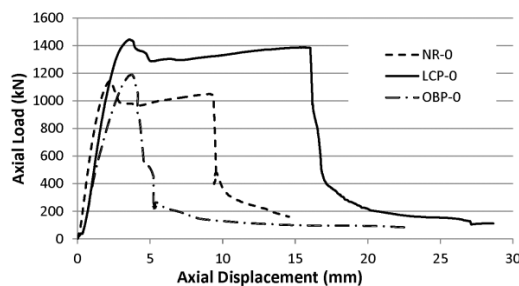
3.4. Ductility of Columns

Ductility is considered as one of the most significant parameters for structural members. In this study, it was determined as the ratio of deflection at 85% of ultimate load after peak and deflection at yield load [17]. Table 3 summaries the ductility of the axially loaded columns devised from the experimental results. It is clear that the two LCP specimens in concentric and 25 mm eccentric loading conditions showed a considerable increase in ductility with 138% and 23%, respectively, compared to the NR specimens. The normalized ductility of Specimen LCP-50 was 0.95, so the ductility of only this specimen was little less than that of the

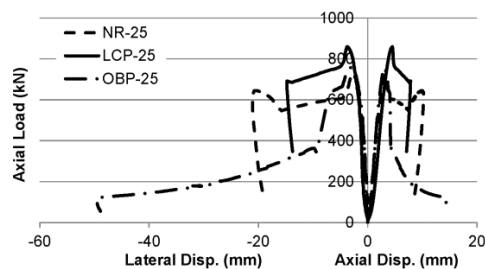
reference column. Specimens OBP-0 and OBP-50 were the most brittle columns compared to the other ones in the concentric and 50 mm eccentric loading conditions, with normalized ductility of 0.62 and 0.81, respectively. However, the remaining specimen in Group OBP indicated higher ductility performance in comparison with the reference specimen, an increase of 10% for Specimen OBP-25.

Table 3. Ductility of axially loaded columns

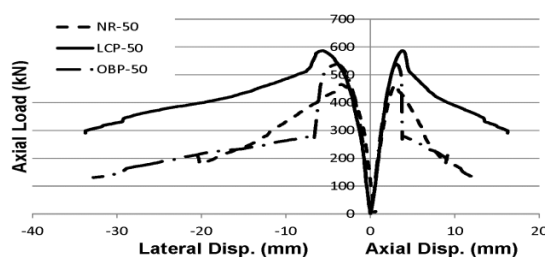
Specimen	Ductility	Normalized Ductility
NR-0	2.35	1
LCP-0	5.59	2.38
OBP-0	1.45	0.62
NR-25	1.37	1
LCP-25	1.68	1.23
OBP-25	1.51	1.10
NR-50	2.01	1
LCP-50	1.90	0.95
OBP-50	1.62	0.81



(a) Concentrically loaded columns



(b) Eccentrically loaded columns, $e = 25$ mm



(c) Eccentrically loaded columns, $e = 50$ mm

Figure 6. Load-deflection diagrams of specimens

4. Conclusions

Based on the experimental program, the following conclusions can be drawn:

- LCP columns demonstrate to be a better design solution than OBP ones with their greater strength and ductility. The good performance of LCP is due to the important role of helical reinforcement, which confines the concrete core and keeps the steel plates stable under loading conditions, especially concentric compression loads.

- The strength and ductility of OBP columns were not as high as expected due to the local buckling of structural steel and premature separation between the cover concrete and the steel core. Buckling of steel plates depends on the distance between the bolts used to connect the steel plates and the presence of lateral reinforcement in the column. Hence, reducing the distance between connection bolts or using lateral steel reinforcement will increase the strength and ductility of the column.

- The applied loading eccentricity visually affects the column load-carrying capacity. Increasing the eccentricity leads to the reduction of ultimate loads of all tested columns, but they must be subjected to more bending moments. It also decreases the normalised ductility of the columns in Group LCP, but increases the normalised ductility for column OBP-25 compared to the remaining columns in this group.

- For utilising these composite columns in building and bridge design, a further study to investigate the scope of using the steel plate and the interaction between steel and concrete needs to be undertaken in detail. In particular, the buckling of steel plate and steel-concrete separation issues, especially Group OBP, are necessary to study as these factors have a significant effect on the strength and ductility of these composite columns.

REFERENCES

- [1] S. R. Razvi and M. Saatcioglu, "Circular high-strength concrete columns under concentric compression", *ACI Structural Journal*, vol. 96, pp. 817-825, 1999.
- [2] M. Hadi, "Behaviour of FRP strengthened concrete columns under eccentric compression loading", *Composite structures*, vol. 77, pp. 92-96, 2007.
- [3] M. N. S. Hadi, "The behaviour of FRP wrapped HSC columns under different eccentric loads", *Composite structures*, vol. 78, pp. 560-566, 2007.
- [4] M. N. S. Hadi and H. Zhao, "Experimental study of high-strength concrete columns confined with different types of mesh under eccentric and concentric loads", *Journal of Materials in Civil Engineering*, vol. 23, pp. 823-832, 2011.
- [5] B. Uy, "Concrete-filled fabricated steel box columns for multistorey buildings: behaviour and design", *Progress in Structural Engineering and Materials*, vol. 1, pp. 150-158, 1998.
- [6] S. El-Tawil and G. G. Deierlein, "Strength and ductility of concrete encased composite columns", *Journal of Structural Engineering*, vol. 125, pp. 1009-1019, 1999.
- [7] S. A. Mirza and T. K. Tikka, "Flexural stiffness of composite columns subjected to major axis bending", *ACI Structural Journal*, vol. 96, pp. 19-28, 1999.
- [8] S. Mirza and E. Lacroix, "Comparative strength analyses of concrete-encased steel composite columns", *Journal of Structural Engineering*, vol. 130, pp. 1941-1953, 2004.
- [9] C. C. Chen and N. J. Lin, "Analytical model for predicting axial capacity and behavior of concrete encased steel composite stub columns", *Journal of Constructional Steel Research*, vol. 62, pp. 424-433, 2006.
- [10] Z. Kala, L. Puklický, A. Omishore, M. Karmazínová, and J. Melcher, "Stability problems of steel-concrete members composed of high-strength materials", *Journal of Civil Engineering and Management*, vol. 16, pp. 352-362, 2010.
- [11] Eurocode-4, "Design of Composite Steel and Concrete Structures - Part 1-1: General Rules and Rules for Buildings", ed. Brussels, Belgium: European Committee for Standardization (CEN), 1994.
- [12] American Institute for Steel Construction, "Load and Resistance Factor Design Specification for Structural Steel Buildings (AISC-LRFD-99)", ed. Chicago: AISC Committee, 1999.
- [13] American Concrete Institute, "Building Code Requirements for Structural Concrete (ACI 318-02)", ed. Detroit: ACI Committee 318, 2002.
- [14] H. Saw and J. Liew, "Assessment of current methods for the design of composite columns in buildings", *Journal of Constructional Steel Research*, vol. 53, pp. 121-147, 2000.
- [15] Australian Standards, "Australian standard for concrete structures (AS 3600-09)", ed. Sydney: Standards Australia, 2009.
- [16] Australian Standards, "Methods of testing concrete - Method of making and curing concrete -- Compression and indirect tensile test specimens (AS 1012.8)", ed. SAI Global InfoStore: Standards Australia, 2000.
- [17] S. Pessiki and A. Pieroni, "Axial Load Behavior of Large Scale Spirally Reinforced High Strength Concrete Columns", *ACI Structural Journal*, vol. 94, pp. 304-313, 1997.

(The Board of Editors received the paper on 22/10/2013,
its review was completed on 11/12/2013)